Crystal Growth of $CuGaSe_2$ Compound for Tandem Photovoltaic Devices

H. Felfli[a], B. Hadjoudja[a,*], A. Khadraoui[a], S. Gagui[a], B. Zaidi[b], B. Chouial[a] and A. Chibani[a]

[a] *Laboratory of Semiconductors, Department of Physics, University Badji Mokhtar, Annaba, Algeria*
[b] *Department of Physics, Faculty of Material Sciences, University of Batna 1, Algeria*

Received: 12.12.2020 & Accepted: 24.03.2021

Doi: 10.12693/APhysPolA.139.655 *e-mail: b_hadjoudja@yahoo.fr

In this work, we have investigated the crystal growth of the $CuGaSe_2$ chalcopyrite structure compound which is intended for tandem photovoltaic devices. Analyses by X-ray diffraction have shown that the obtained ingots are polycrystalline and have a chalcopyrite structure. The preferential orientation along the plane (112) — very suitable for photovoltaic conversion — was obtained. The lattice parameters a and c were calculated from the X-ray spectra, the ratio c/a was found to be near to 2. The use of an energy dispersive spectrometer (EDS) for the analysis of the chemical composition of the constituents showed that the investigated sample had a stoichiometric ratio Cu/In = 0.99. The morphological analysis performed using a scanning electron microscope (SEM) has shown that the $CuGaSe_2$ compound has a well-crystallized appearance with an average grain size of about 3 μm. Characterizations by Hall effect measurements and resistivity have shown that the prepared ingot exhibits a p-type conductivity and low resistivity, of the order of 12.73 Ω cm. The measurement of the photoconductivity of the prepared compound has allowed us to determine the value of the gap at room temperature. The gap was found to be near 1.68 eV. The results obtained within the framework of this study have shown that the prepared $CuGaSe_2$ compound has good crystalline and optoelectronic properties, which makes it one of the ideal compounds to be used as the top cell for a tandem photovoltaic device.

topics: $CuGaSe_2$, crystal growth, synthesis, tandem photovoltaic device

1. Introduction

In researches on solar cells based on materials with a chalcopyrite structure Cu(Ga,In)Se_2 (CIGS), a photovoltaic conversion is of great interest [1–13]. The CIGS compounds have a direct gap and an absorption power greater than silicon [14]. This results in a lesser amount of useful material, and a significant reduction in manufacturing costs. Efficiencies higher than 22.6% were obtained [15]. Therefore, the ternary compound $CuGaSe_2$ (CGS) of chalcopyrite structure is considered as a very promising absorber material for the top cell in a CIGS tandem structure [16–18], given its suitable band gap energy (1.68 eV), process compatibility with a CIGS bottom cell, and complete miscibility of CIGS. This material is distinguished by a high absorption coefficient and a direct transition gap. Efficiency higher than 25% of thin-film tandem solar cells is predicted as a very attractive way forward in the photovoltaic technology [19, 20]. Crystals of the $CuGaSe_2$ compound have been a subject of intensive investigation for many years [21–25]. Ingots of the ternary compound $CuGaSe_2$, free of microcracks and voids, can be readily grown by the Bridgman method. In this work, we used a technique inspired by the vertical Bridgman method [26] to prepare and study the structural, electrical and optical properties of $CuGaSe_2$.

2. Materials and methods

2.1. Fabrication conditions

We desire to obtain a compound with the following proportions: 25% of copper, 25% of gallium and 50% of selenium. The elements Cu, Ga and Se are used as small balls of a consistent purity: 5N for copper and 6N for gallium and selenium. We keep the same proportions for the mixture, and its elements will be weighed with the ratio of their molar mass.

The most difficult to handle is the reference material for weighing. In the case of CGS, the gallium seems to be the least handy (mainly because of its low melting point) and therefore Ga

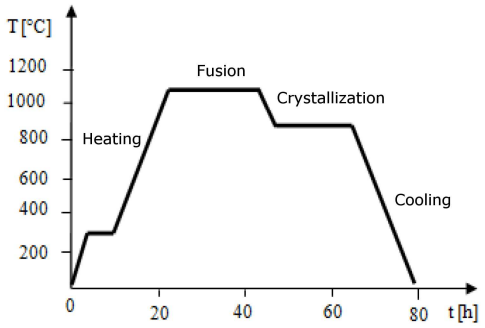

Fig. 1. Optimized thermal cycle for the preparation of the $CuGaSe_2$ compound.

TABLE I

Weighing of the elements of the $CuGaSe_2$ compound.

Proportions [%]			Weighed masses [g]			Total
Cu	Ga	Se	M(Cu)	M(Ga)	M(Se)	mass [g]
25	25	50	1.3898	1.6962	2.9575	6.0435

is used as the reference for the other two elements. Once the amount of gallium is chosen, the amounts of the two other elements will be calculated using the following recipes:

$$M(\mathrm{Cu}) = \frac{M(\mathrm{Ga}) \times \text{molar mass of Cu}}{\text{molar mass of Ga}} \quad (1)$$

and

$$M(\mathrm{Se}) = \frac{2M(\mathrm{Ga}) \times \text{molar mass of Se}}{\text{molar mass of Ga}}. \quad (2)$$

The weighings were carried out with a high precision electronic balance (10^{-4} g). The weighing results are reported in Table I.

The quartz tube which was meant to receive the mixture of three elements was pre-cleaned for 30 min with a mixture of hydrofluoric acid (HF), nitric acid (HNO_3) and deionized water (H_2O) in the proportions 2, 3, 5. After being rinsed with deionized water, the tube was dried in an oven at 80 °C for 3 h. The quartz tube was then loaded with the mixture of the three elements and sealed under a vacuum of 10^{-6} Torr. The tube was placed inside the furnace at a position set in advance by calibration to receive the maximum energy.

After sealing, the tube was placed in an oven where it was subjected to an optimized thermal cycle composed of seven steps as shown in Fig. 1.

2.2. Characterization techniques

The structural properties of the obtained ingot were determined by an X-ray diffraction (XRD) diffractometer, operating with CoK_α radiation with the wavelength $\lambda = 1.54051$ Å. In addition, a scanning electron microscope (SEM) combined with an energy dispersive spectrometer (EDS) was used to examine the morphology of the ingot and to determine the chemical composition of its constituents. Electrical properties were determined at room temperature by a Hall effect measurement system (HMS 3000). Absorption measurements were performed at room temperature using a Cary 5000 UV-Vis-NIR spectrophotometer at a scanning rate of 200 nm/min in the 200–1200 nm wavelength range.

3. Results and discussion

At the end of the thermal cycle that lasts 80 h, we took the quartz tube out of the furnace, and the formed product was retrieved. The obtained $CuGaSe_2$ sample presented a complete solidification and good morphology as shown in Fig. 2.

3.1. Structural properties

Analyses by X-ray diffraction have permitted us to study the crystal structure of the obtained $CuGaSe_2$ ingots and to determine different crystallization planes as well as different phases. The X-ray spectrum of the sample shows the presence of a peak, indicating a very strong preferential orientation of growth in the direction (112). This can be seen in Fig. 3. Alongside this orientation, doublets are apparent: ((220) (204)), ((312) (116)), ((400) (008)), ((332) (316)) and ((424) (228)). The plane (112) is the most intense preferential orientation located at $2\theta = 27.7°$. Notably, Kanan et al. [27] indicated that the planes having (112) orientation are very desirable for the photovoltaic conversion.

Fig. 2. The $CuGaSe_2$ sample presenting a complete solidification.

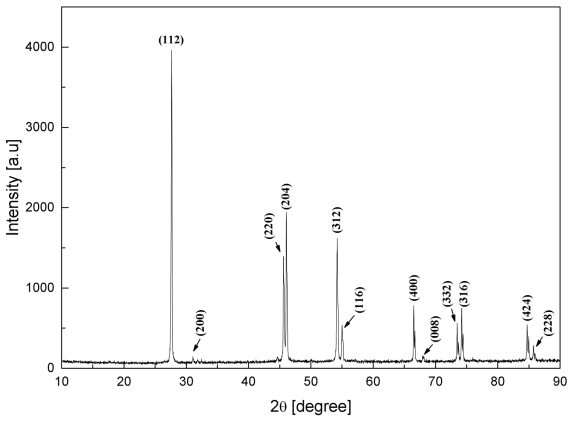

Fig. 3. X-ray diffraction spectrum of the bulk $CuGaSe_2$.

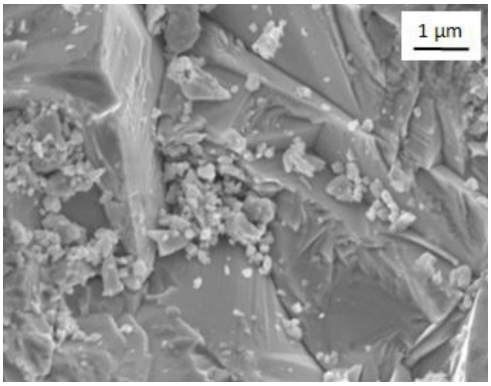

Fig. 4. Morphology of the $CuGaSe_2$ compound.

TABLE II

Atomic composition of the $CuGaSe_2$ compound.

Cu [%]	Ga [%]	Se [%]	Cu/Ga
24.93	25.22	49.85	0.99

From the X-ray spectrum of the prepared $CuGaSe_2$ compound, we have calculated the lattice parameters a and c. The values obtained are $a = 5.56$ Å and $c = 11.07$ Å. The presence of doublets ((220) (204)) and ((312) (116)), on the one hand, and the preferential orientation (112), on the other hand, show that the obtained ingot is polycrystalline and is of a chalcopyrite type structure.

3.2. Morphology and chemical composition

A scanning electron microscope (SEM) combined with an energy dispersive spectrometer (EDS) was used to examine the morphology of the ingot and to determine the chemical composition of its constituents. Due to the morphological analysis one can state that the $CuGaSe_2$ compound has a well-crystallized appearance with an average grain size of about 3 μm, as indicated in Fig. 4. The atomic composition of the constituents was obtained by EDS, after an analysis of five different places of the $CuGaSe_2$ ingot. The result showed that a stoichiometric ratio of this sample was equal to Cu/In= 0.99 — as reported in Table II.

3.3. Electrical properties

To determine the electrical characteristics of $CuGaSe_2$, we used the HMS 3000. The results are summarized in Table III. They prove that the prepared sample has a low resistivity, good mobility and p-type conductivity. The type of conductivity obtained for this compound is desirable for the manufacture of solar cells [28].

3.4. Optical properties

Optical analysis of the prepared $CuGaSe_2$ compound was performed at room temperature by a Cary 5000 UV-Vis-NIR spectrophotometer.

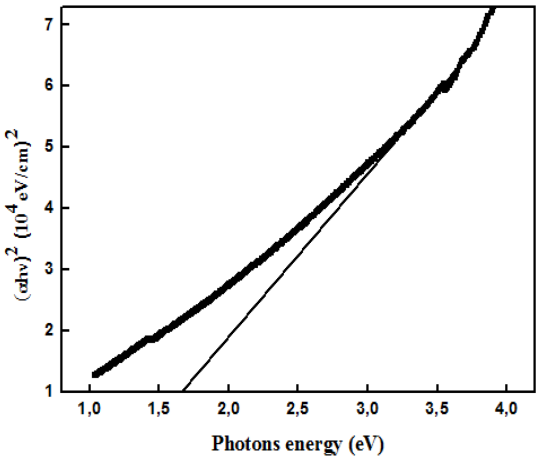

Fig. 5. Plot of $(\alpha h\nu)^2$ versus photons energy $h\nu$ of the $CuGaSe_2$ compound.

TABLE III

Electrical characteristics of the $CuGaSe_2$ compound.

type of conductivity	resistivity [Ωcm]	mobility [cm^2/(Vs)]	concentration of carriers [cm^{-3}]
p	12.73	6.14	7.99×10^{16}

In Fig. 5, we have presented the variation of $(\alpha h\upsilon)^2$ as a function of the photons energy $h\upsilon$ for the $CuGaSe_2$ compound prepared in the framework of this study. Using this characteristic, we seek to determine the value of the band gap energy of the investigated compound.

The band gap energy E_g can be obtained by the following procedure [29]: (i) a dependence $(\alpha h\upsilon)^2$ versus photons energy $(h\upsilon)$ is plotted; (ii) a tangent line is obtained by extrapolating the curve of $(\alpha h\upsilon)^2$ vs. $h\upsilon$; and (iii) the tangent line is extended to intersect with the abscissa axis. Then, the band gap energy E_g is obtained at $(\alpha h\upsilon)^2 = 0$. It can be seen (Fig. 5) that the band gap of the prepared material is close to 1.68 eV. This value is in good agreement with that reported in [30, 31]. Theoretical studies have shown that an ideal top cell in the tandem configuration should have a band gap of 1.70 eV [19]. Because of this requirement, $CuGaSe_2$ with a bulk band gap near to 1.68 eV, as the one obtained in this study, can be considered as a suitable absorber for the top cell of tandem photovoltaic devices.

4. Conclusion

We are interested in the synthesis of the $CuGaSe_2$ compound using a technique inspired by the Bridgman method. The obtained ingots after the optimization of the preparation parameters have a good morphology. Analyses by X-ray diffraction showed that the obtained $CuGaSe_2$ compound crystallizes as the chalcopyrite form, with a preferential direction (112) and the lattice parameters $a = 5.56$ Å

and $c = 11.07$ Å. With an energy dispersive spectrometer (EDS) used for the analysis of the chemical composition of the constituents we have obtained for this sample, a stoichiometric ratio Cu/In = 0.99. The morphological analysis performed by the scanning electron microscope (SEM) showed that the $CuGaSe_2$ compound has a well-crystallized appearance with an average grain size of about 3 μm. Electrical characterization by Hall and resistivity measurements allowed us to see that the obtained sample has a p-type conductivity with low resistivity, on the order of 12.73 Ω cm. In addition, analyses by the spectrophotometer confirmed a good absorption spectrum of the prepared compound and subsequently determined the gap width which was found to be close to 1.68 eV.

Our studies have proved the good optoelectronic properties of the prepared $CuGaSe_2$ compound. This makes it one of the ideal compounds to be used as the top cell for tandem photovoltaic devices.

References

[1] S. Ishizuka, P.J. Fons, *J. Cryst. Growth* **532**, 125407 (2020).

[2] B. Zaidi, M. Zouagri, S. Merad, C. Shekhar, B. Hadjoudja, B. Chouial, *Acta Phys. Pol. A* **136**, 988 (2019).

[3] S. Siebentritt, *Curr. Opin. Green Sustain. Chem.* **4**, 1 (2017).

[4] P. Tsoulka, A. Rivalland, L. Arzel, N. Barreau, *Thin Solid Films* **709**, 138224 (2020).

[5] A. Khadir, *Acta Phys. Pol. A* **137**, 1128 (2020).

[6] M. Schmid, R. Klenk, M.C. Lux-Steiner, *Sol. Energy Mater. Sol. Cells* **93**, 874 (2009).

[7] E. Jarzembowski, M. Maiberg, F. Obereigner, K. Kaufmann, S. Krause, R. Scheer, *Thin Solid Films* **576**, 75 (2015).

[8] H.J. Jo, D.H. Jeon, B.S. Ko, S.J. Sung, D.K. Hwang, J.K. Kang, D.H. Kim, *Curr. Appl. Phys.* **14**, 318 (2014).

[9] H.M. Friedlmeier, P.M. Pérez, I. Klugius, P. Jackson, O. Kiowski, E. Ahlswede, M. Powalla, *Thin Solid Films* **535**, 92 (2013).

[10] D. Nam, S. Jung, S. Ahn, J. Gwak, K. Yoon, J.H. Yun, H. Cheong, *Thin Solid Films* **535**, 118 (2013).

[11] L. Kranz, A. Abate, T. Feurer, F. Fu, E. Avancini, J. Lockinger, P. Reinhard et al., *J. Phys. Chem. Lett.* **6**, 2676 (2015).

[12] S. Ishizuka, *Phys. Status Solidi A* **216**, 1800873 (2019).

[13] P. Jackson, D. Hariskos, R. Wuerz, O. Kiowski, A. Bauer, T.M. Friedlmeier, M. Powalla, *Phys. Status Solidi RRL* **9**, 28 (2015).

[14] J. Jaffe, A. Zunger, *Phys. Rev. B* **29**, 1882 (1984).

[15] P. Jackson, R. Wuerz, D. Hariskos, E. Lotter, W. Witte, M. Powalla, *Phys. Status Solidi RRL* **10**, 583 (2016).

[16] O. Schenker, M. Klenk, E. Bucher, *Thin Solid Films* **361–362**, 454 (2000).

[17] D. Fischer, N. Meyer, M. Kuczmik, M. Beck, A. Jager-Waldau, M.Ch. Lux-Steiner, *Sol. Energy Mater. Sol. Cells* **67**, 105 (2001).

[18] M. Rusu, S. Wiesner, D.F. Marron, A. Meeder, S. Doka, W. Bohne, S. Lindner et al., *Thin Solid Films* **451-452**, 556 (2004).

[19] T.J. Coutts, J.S. Ward, D.L. Young, K.A. Emery, T.A. Gessert, R. Noufi, *Prog. Photovolt. Res. Appl.* **11**, 359 (2003).

[20] M. Elbar, S. Tobbeche, A. Merazga, *Solar Energy* **122**, 104 (2015).

[21] X. Hu, J. Xue, J. Tian, G. Weng, S. Chen, *Appl. Opt.* **56**, 2330 (2017).

[22] J. Bekaert, R. Saniz, B. Partoens, D. Lamoen, *J. Appl. Phys.* **117**, 015104 (2015).

[23] D.W. Houck, S.V. Nandu, T.D. Siegler, B.A. Korgel, *ACS Appl. Nano Mater.* **2**, 4673 (2019).

[24] H. Benzaghoua, A.E. Merada, T. Ouahranib, M.R. Boufataha, *Optik* **174**, 27 (2018).

[25] M. Ider, *Int. J. Electrochem. Sci.* **15**, 9049 (2020).

[26] L. Djellal, A. Bouguelia, M. Kadi Hanifi, M. Trari, *Sol. Energy Mater. Sol. Cells* **92**, 594 (2008).

[27] M.D. Kannan, R. Balasundaraprabhu, S. Jayakumar, P. Ramanathaswamy, *Sol. Energy Mater. Sol. Cells* **81**, 379 (2004).

[28] M. Venkatachalam, M.D. Kannan, S. Jayakumar, R. Balasundaraprabhu, N. Muthukumarasamy, *Thin Solid Films* **516**, 6848 (2008).

[29] A.E. Morales, E.S. Mora, U. Pal, *Rev. Mex. de Fis.* **53**, 18 (2007).

[30] M. Rusu, S. Doka, C.A. Kaufmann, N. Grigorieva, Th. Schedel-Niedrig, M.Ch. Lux-Steiner, *Thin Solid Films* **480**, 341 (2005).

[31] J. Stankiewicz, W. Giriat, J. Ramos, M.P. Vecchi, *Sol. Energy Mater. Sol. Cells* **1**, 369 (1979).